Table 1 - Flowchart of a numerical procedure for multi-body optimum design of 3R manipulators.

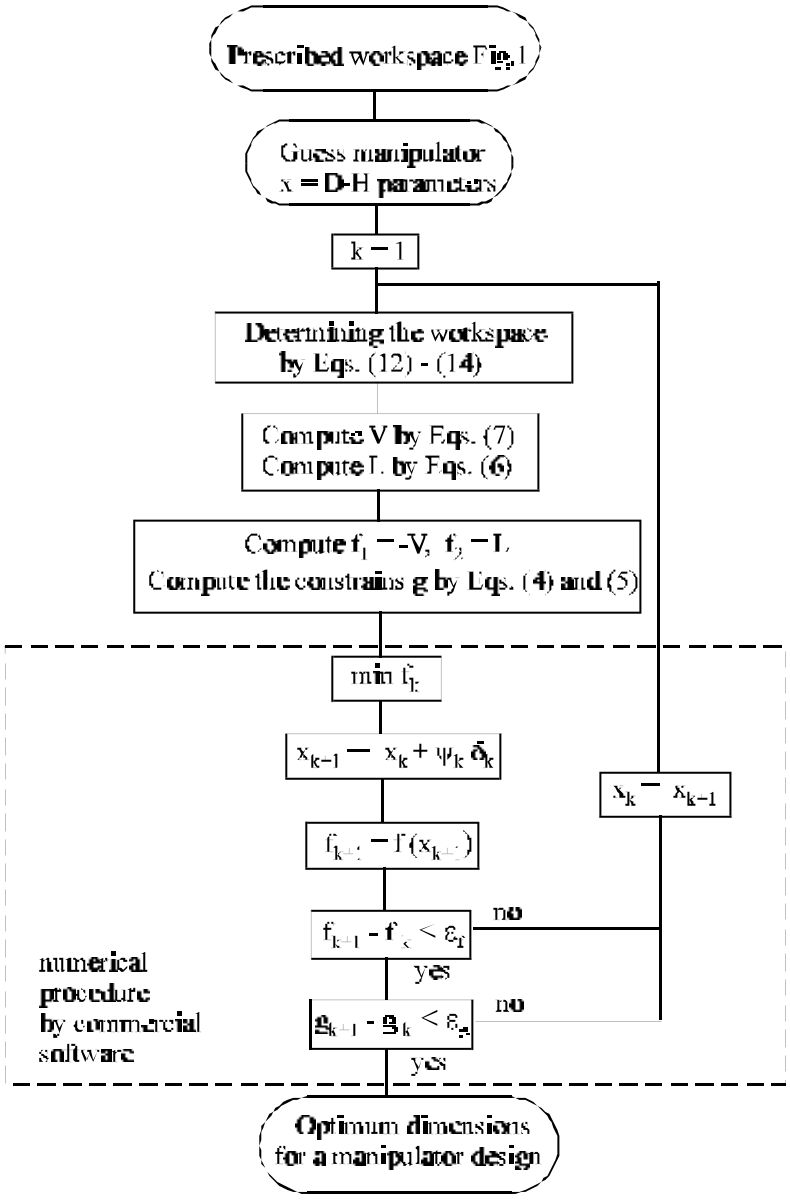

The Ring equations in 3.1.2.1 are useful to express analytically the constraint Eqs.(3.193) as explicit functions of the design parameters. In addition, these equations are useful to calculate analytically the derivatives, which are involved in the numerical optimization process.

for example the first derivatives with respect to the design parameter a_1 can be expressed in the form

$$\frac{\partial r_{1,j}}{\partial a_1}=\frac{1}{2r_{1,j}}\left[\frac{\partial A_1}{\partial a_1}-2z_{1,j}\frac{\partial z_{1,j}}{\partial a_1}-\frac{\left(C_1 z_{1,J}+D_1\right)G_1+F_1}{E_1^2}\frac{\partial E_1}{\partial a_1}\right]+ +\frac{1}{2r_{1,j}E_1}\left[\frac{\partial F_1}{\partial a_1}+\frac{\partial G_1}{\partial a_1}\left(C_1 z_{1,J}+D_1\right)+G_1\left(\frac{\partial D_1}{\partial a_1}+z_{1,J}\frac{\partial C_1}{\partial a_1}+C_1\frac{\partial z_{1,j}}{\partial a_1}\right)\right] \tag{3.1.94}$$

$$\frac{\partial z_{1,j}}{\partial a_1}=-\frac{z_{1,j}}{C_1}\frac{\partial C_1}{\partial a_1}-\frac{-L_1\pm Q_1^{1/2}}{K_1^2 C_1}\frac{\partial K_1}{\partial a_1}+\frac{1}{K_1 C_1}\left(\pm\frac{1}{2Q_1}\frac{\partial Q_1}{\partial a_1}-\frac{\partial L_1}{\partial a_1}-K_1\frac{\partial D_1}{\partial a_1}\right) \tag{3.1.95}$$

$$\frac{\partial u_j}{\partial a_1}=\mp\frac{1}{2}\left[\frac{\partial A_1}{\partial a_1}-\left(\frac{-L_1\pm Q_1^{1/2}}{E_1^2 K_1}+\frac{F_1}{E_1^2}\right)\frac{\partial E_1}{\partial a_1}-\frac{-L_1\pm Q_1^{1/2}}{K_1^2 E_1}\frac{\partial K_1}{\partial a_1}+\frac{1}{E_1}\frac{\partial F_1}{\partial a_1}\right]-\frac{1}{2K_1 E_1}\left(\frac{\partial L_1}{\partial a_1}\pm\frac{1}{2Q_1^{1/2}}\frac{\partial Q_1}{\partial a_1}\right) \tag{3.1.96}$$

$$\frac{\partial V}{\partial a_1}=\sum_1^N\frac{\pi}{2}\left[\left(\frac{\partial z_{1,n+1}}{\partial a_1}+\frac{\partial z_{1,n}}{\partial a_1}\right)\left(r_{1,n}^2-r_{1,n+1}^2\right)+2\left(z_{1,n+1}+z_{1,n}\right)\left(r_{1,n}\frac{\partial r_{1,n}}{\partial a_1}-r_{1,n+1}\frac{\partial r_{1,n+1}}{\partial a_1}\right)\right] \tag{3.1.97}$$

Higher derivatives can be obtained by further differentiating the above expressions and using the algebraic formulation in 3.1.3.2.

An example is illustrated in Fig.3.22.
the algorithm reaches a feasible solution with few iterations (12!) and it optimizes the workspace with a manipulator length of 11.89 a_1 and a volume of 1000.34 a_1^3.

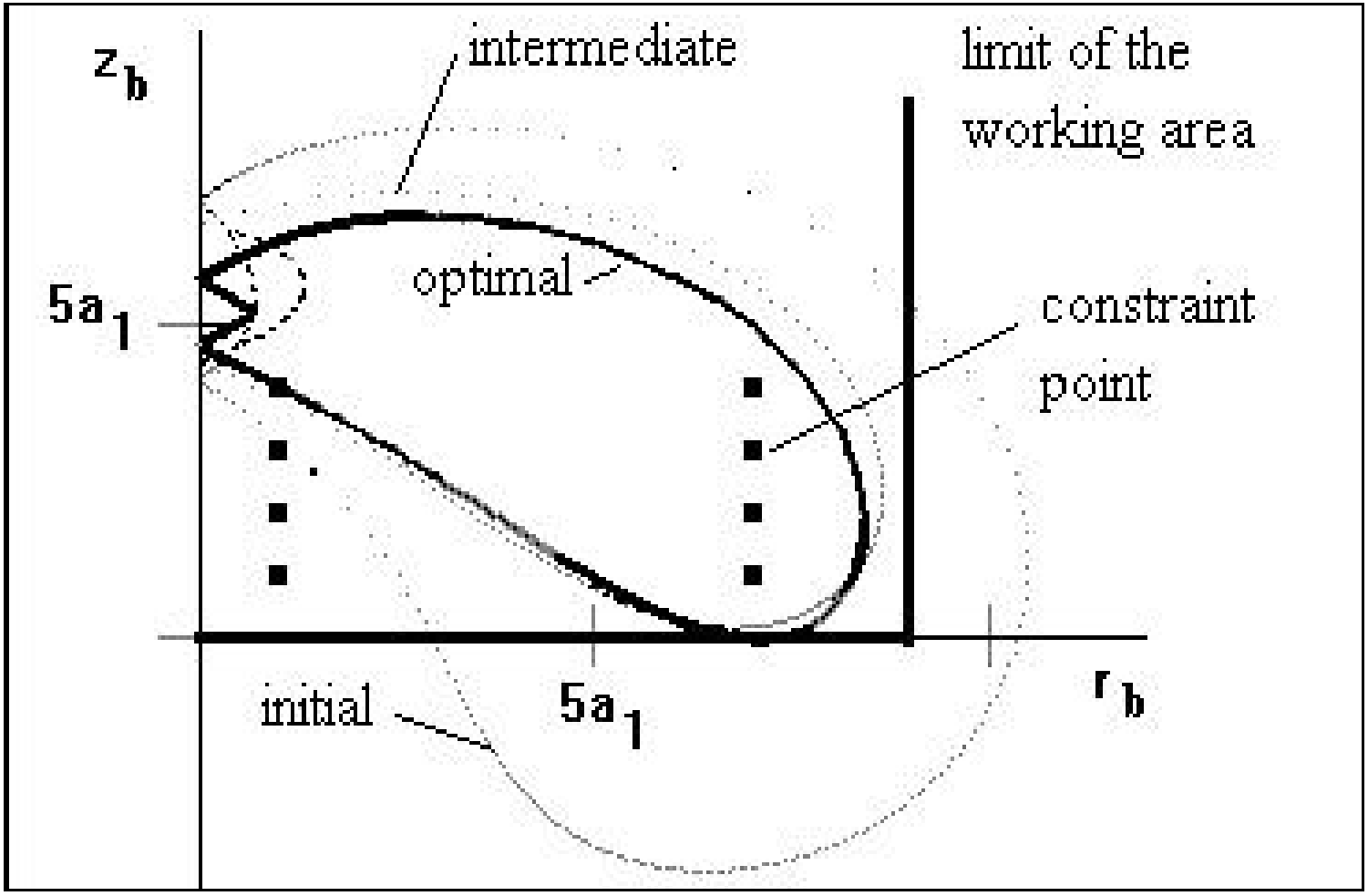

Fig.3.22: An example of optimum design evolution for 3R manipulator with prescribed workspace.

a multi-objective optimization problem in the form

$$\min f_1 = -V$$
$$\min f_2 = L \qquad (3)$$

subject to

$$g_1 = z_{min} \geq z_{0,min}$$
$$g_2 = r_{min} \geq r_{0,min}$$
$$g_3 = r_{max} \leq r_{0,max} \qquad (4)$$
$$g_4 = z_{max} \leq z_{0,max}$$

and

$$g_5 = Area \geq Area_0$$
$$g_6 = a_3 / a_1 \geq K_0 \qquad (5)$$
$$g_7 = a_3 - (a_2 + d_2 \tan \alpha_2) \leq 0$$

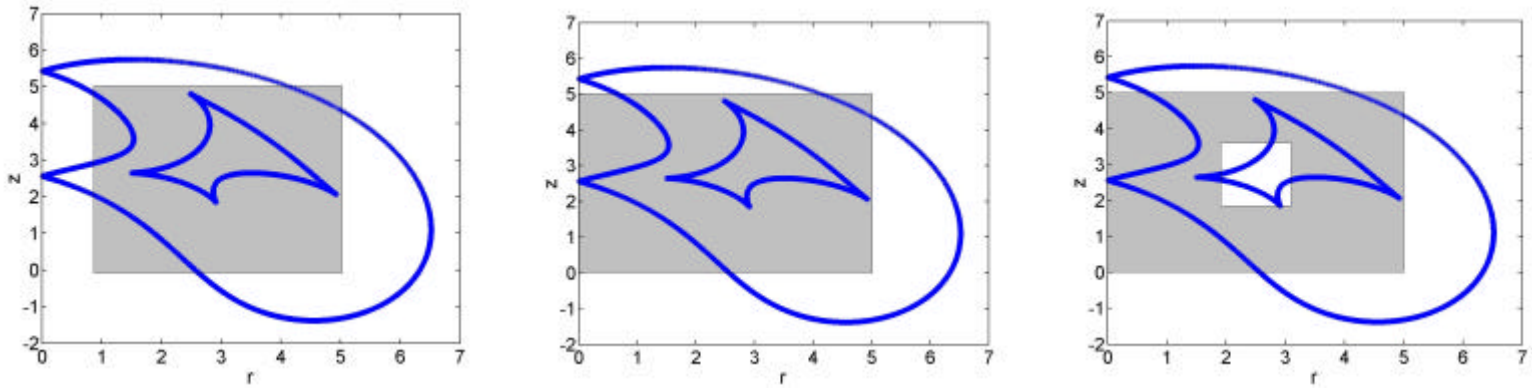

Fig.4 Initial guess for the test of the optimum design of a 3R manipulator in the case: a) with hole and without void; b) without hole and void; c) without hole and with void.

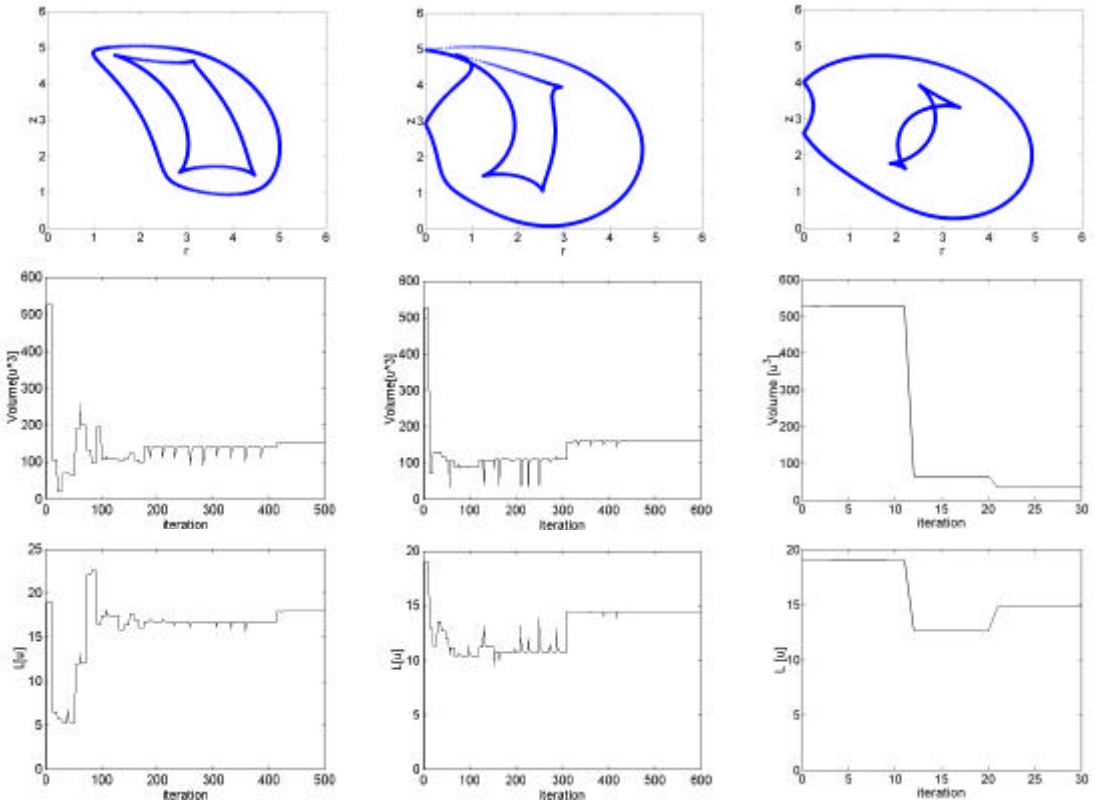

a) b) c)

Fig.5 Results of the optimum design of 3R manipulator in term of obtained workspace cross-section (first row), evolution of objective functions volume V (second row) and manipulator size L (third row) as a function of the design prescribed in Fig.4 : a) with hole and without void; b) without hole and without void; c) without hole and with void.

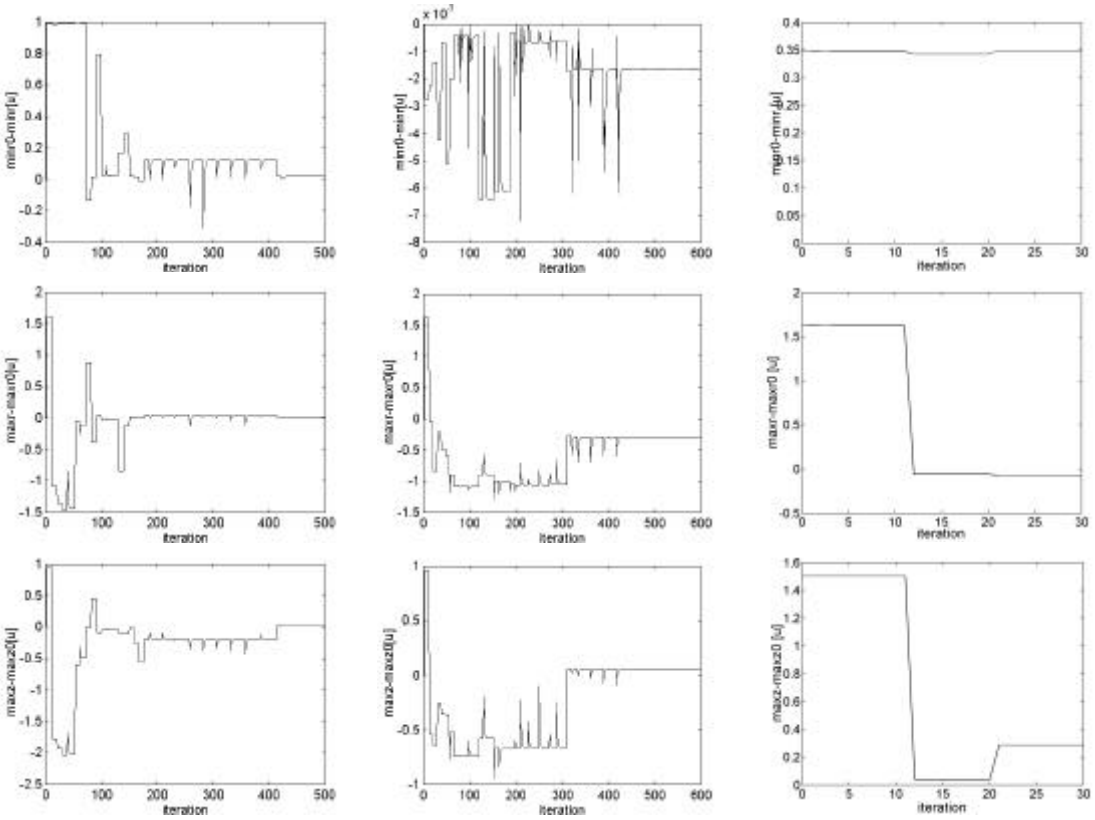

a) b) c)

Fig.6 Numerical evolution of the constraints in Eqs. (2) during the optimization process for the cases of Fig.5: a) with hole and without void; b) without hole and void; c) without hole and with void.

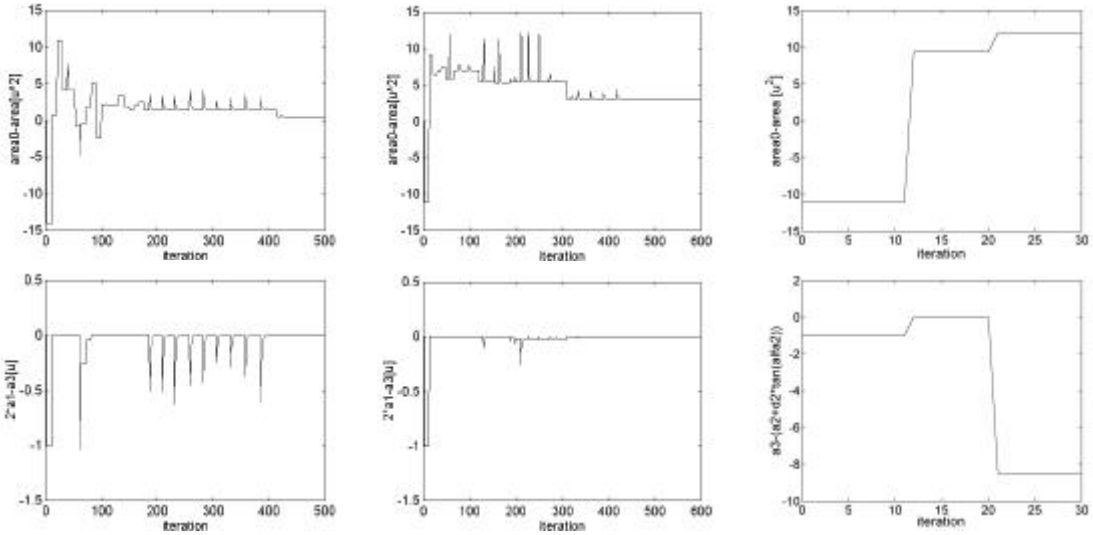

Fig.7 Results of the evolution of the additional constraints in Eqs. (5) during the optimization process for the case of Fig.5: a) with hole and void; b) without hole and void; c) without hole and with void.

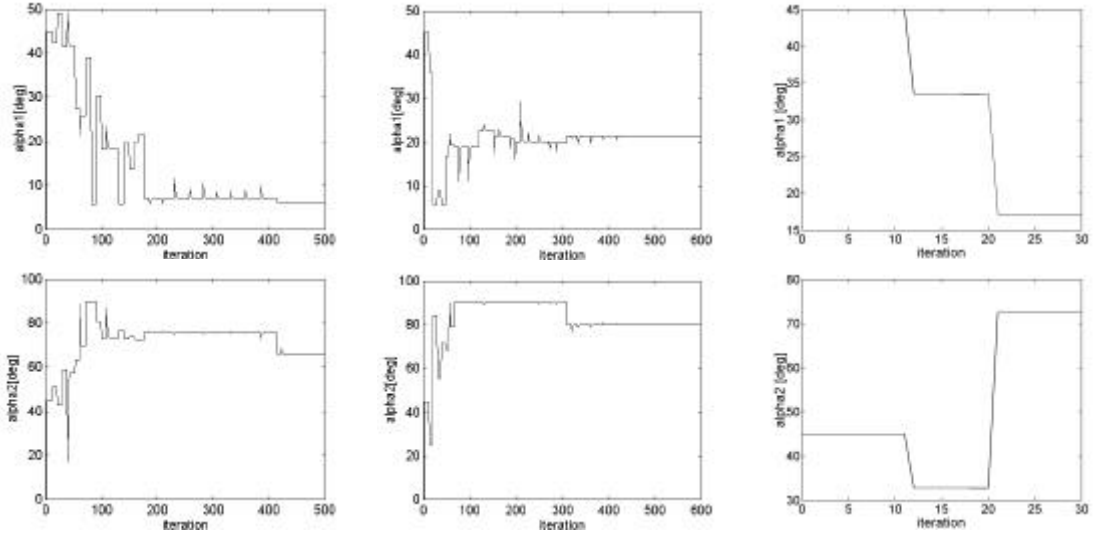

a) b) c)

Fig.8 Results of the evolution of design parameters α_1 and α_2 during the optimization process for the case of Fig.5: a) with hole and without void; b) without hole and void; c) without hole and with void.

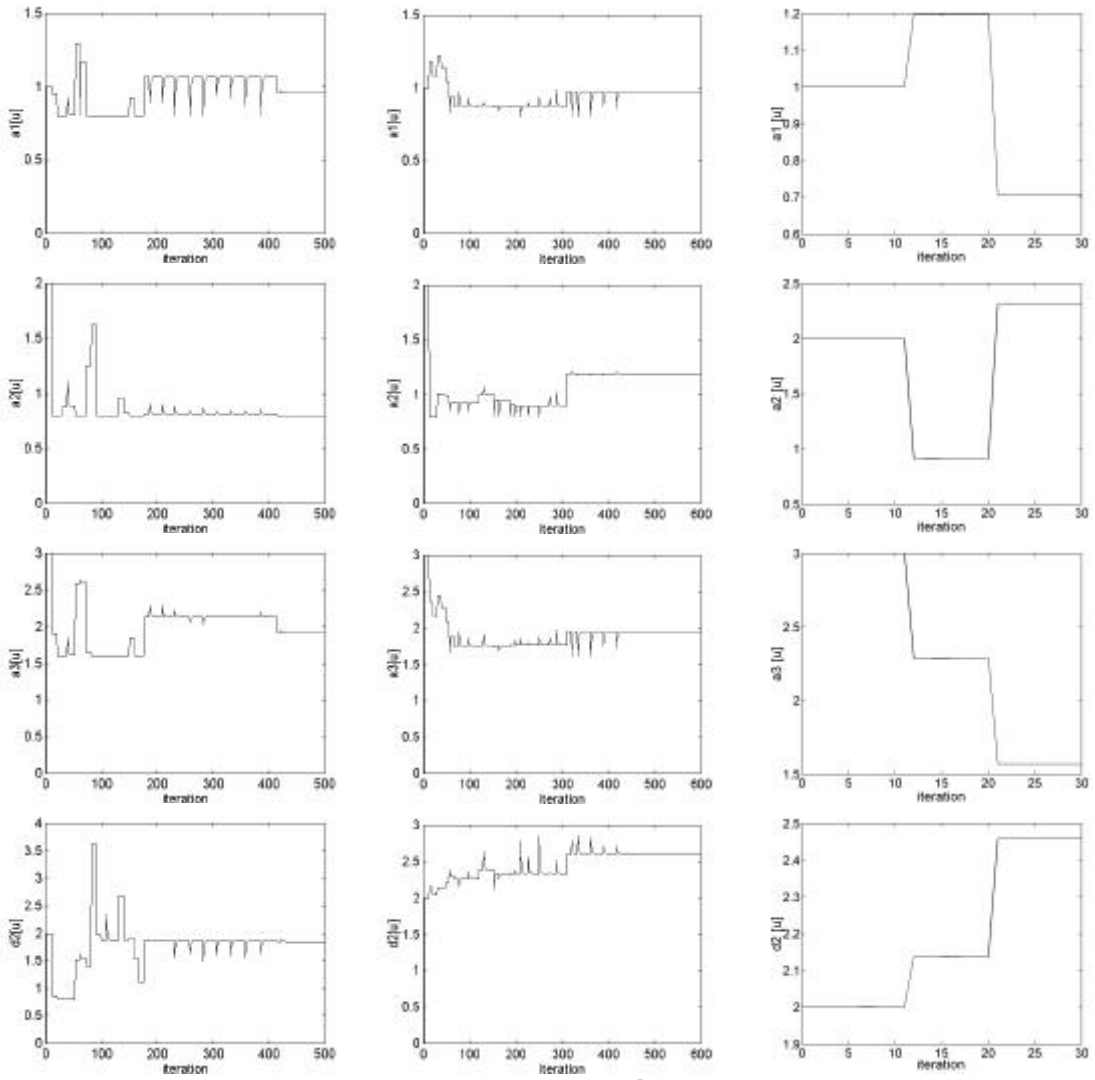

a) b) c)

Fig.9 Results of the evolution of design parameters a_1, a_2, a_3, d_2, d_3 during the optimization process for the case of Fig.5: a) with hole and without void; b) without hole and void; c) without hole and with void.

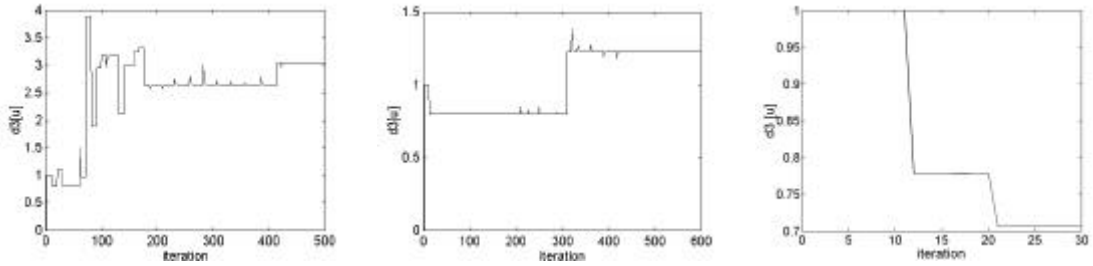

a) b) c)

Fig.9 Results of the evolution of design parameters a_1, a_2, a_3, d_2, d_3 during the optimization process for the case of Fig.5: a) with hole and without void; b) without hole and void; c) without hole and with void.

Table 2 - Numerical results for the multi-objective functions for the design cases of Figs.4 and 5. (Dimension are expressed in u unit length)

Objective Function	$V(u^3)$	L(u)	Iteration number
Initial	555.750	19.000	-
Case a)	153.727	17.960	432
Case b)	161.749	14.484	554
Case c)	34.179	14.833	21

Table 3 - Numerical results for the constraints in Figs.6 and 7 (Dimensions are in u unit length)

Constraints	g_1 (u)	g_2 (u)	g_3 (u)	g_4 (u)	g_5 (u^2)	g_6 (u)	g_7 (u)
Initial	3.466	0.999	0.622	-0.047	-11.379	-1.000	Not used
Case a)	-2.440	0.017	0.007	0.037	0.491	0.000	Not used
Case b)	-0.076	-0.002	-0.294	0.055	3.046	0.000	Not used
Case c)	-0.304	0.348	-0.074	0.287	11.963	Not used	-8.514

Table 4 - Numerical results for the design parameters in Figs.8 and 9 (Dimensions are in u unit length)

Design parameters	a_1 (u)	a_2 (u)	a_3 (u)	d_2 (u)	d_3 (u)	α_1 (deg)	α_2 (deg)
Initial	1.000	2.000	3.000	2.000	1.000	44.977	44.977
Case a)	0.957	0.800	1.913	1.847	3.055	6.073	66.1184
Case b)	0.971	1.193	1.943	2.613	1.232	21.371	80.041
Case c)	0.706	2.310	1.568	2.458	0.706	17.131	74.478

10. Extension to parallel manipulators

- $$i = \left[\frac{x + \Delta x}{x}\right]; \qquad j = \left[\frac{y + \Delta y}{y}\right] \qquad (3)$$

$$P_{ij} = \begin{cases} 0 \text{ if } P_{ij} \notin \mathrm{W(H)} \\ 1 \text{ if } P_{ij} \in \mathrm{W(H)} \end{cases} \qquad (4)$$

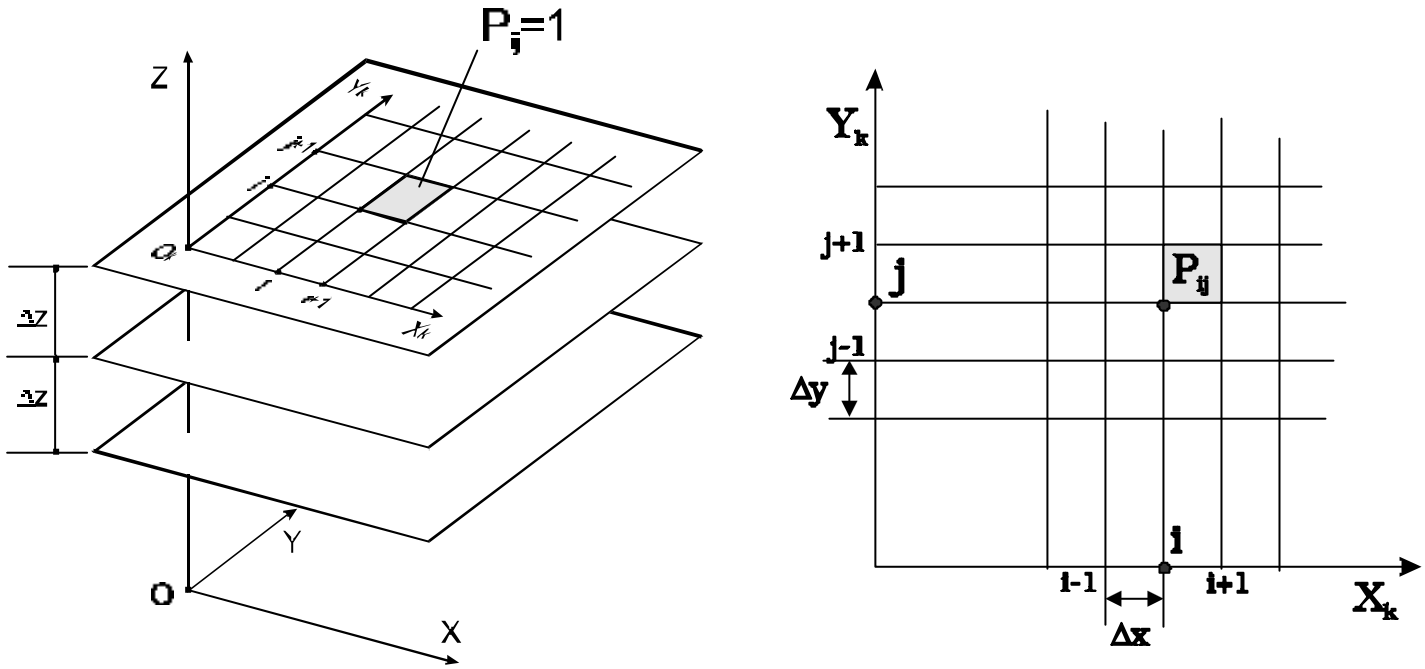

Figure 16 A scheme for binary representation and evaluation of manipulator workspace.

$$A_z = \sum_{i=1}^{i_{max}} \sum_{j=1}^{j_{max}} \left(P_{ij}\ \Delta x\, \Delta y\right) \qquad (5)$$

$$V = \sum_{z=z_{min}}^{z=z_{max}} A_z\ \Delta z \qquad (6)$$

An example: CAPAMan (Cassino Parallel Manipulator)

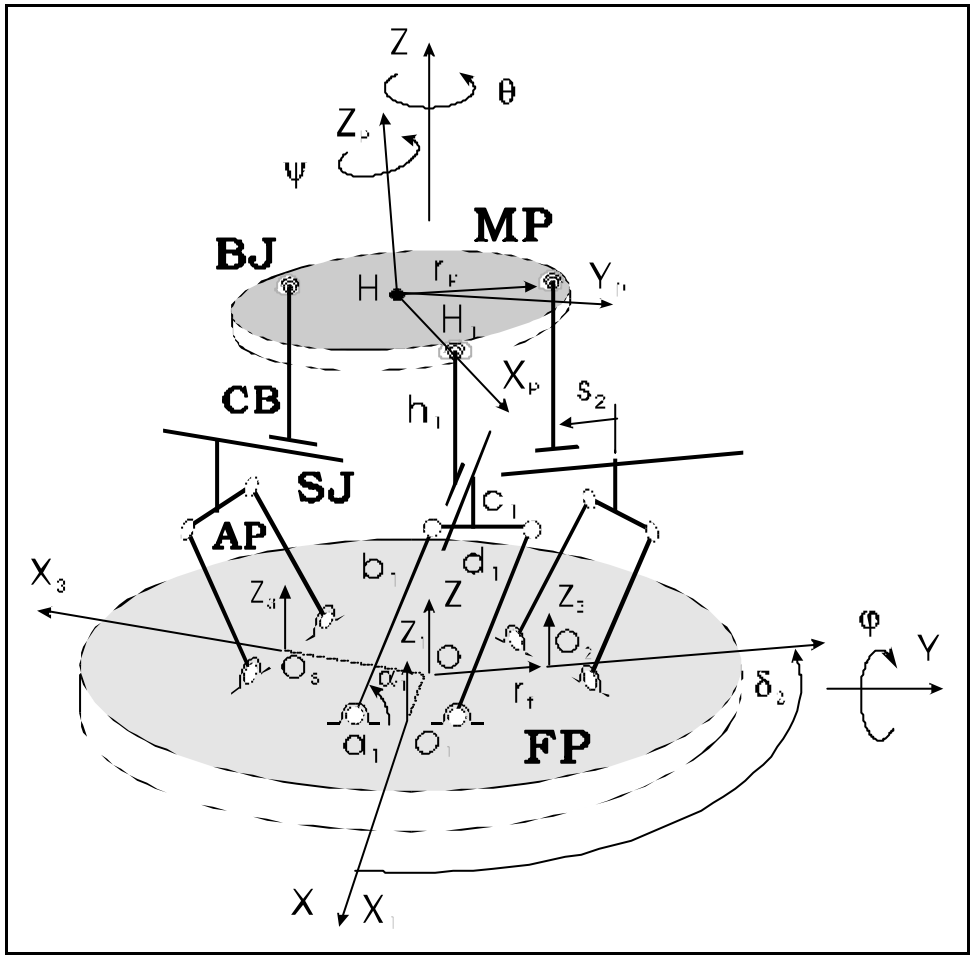

Fig.3.41: Kinematic chain and design parameters of CaPaMan.

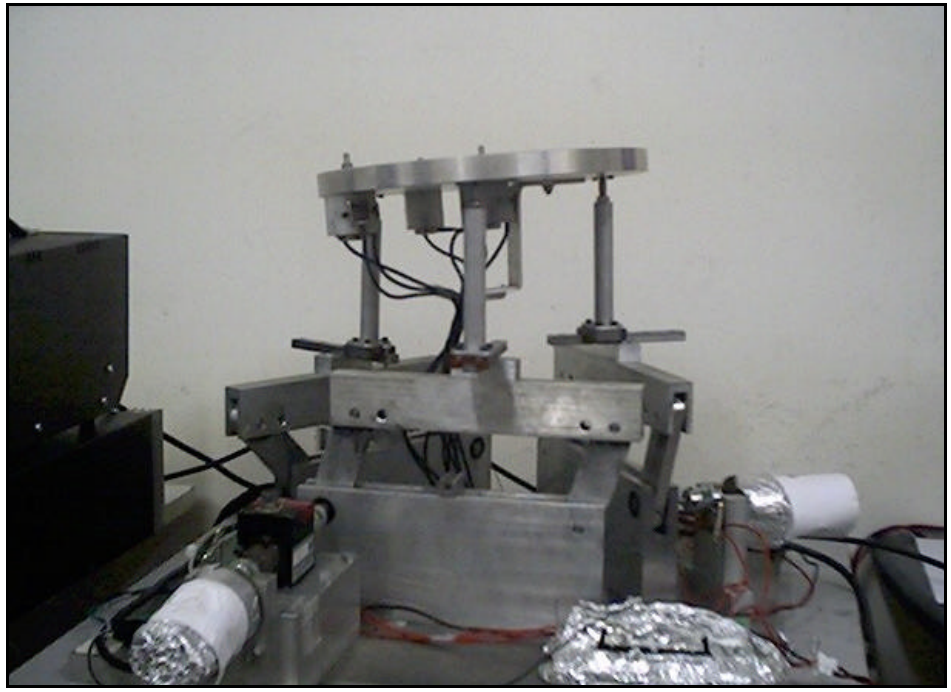

Fig.3.42: A built prototype at LARM in Cassino.

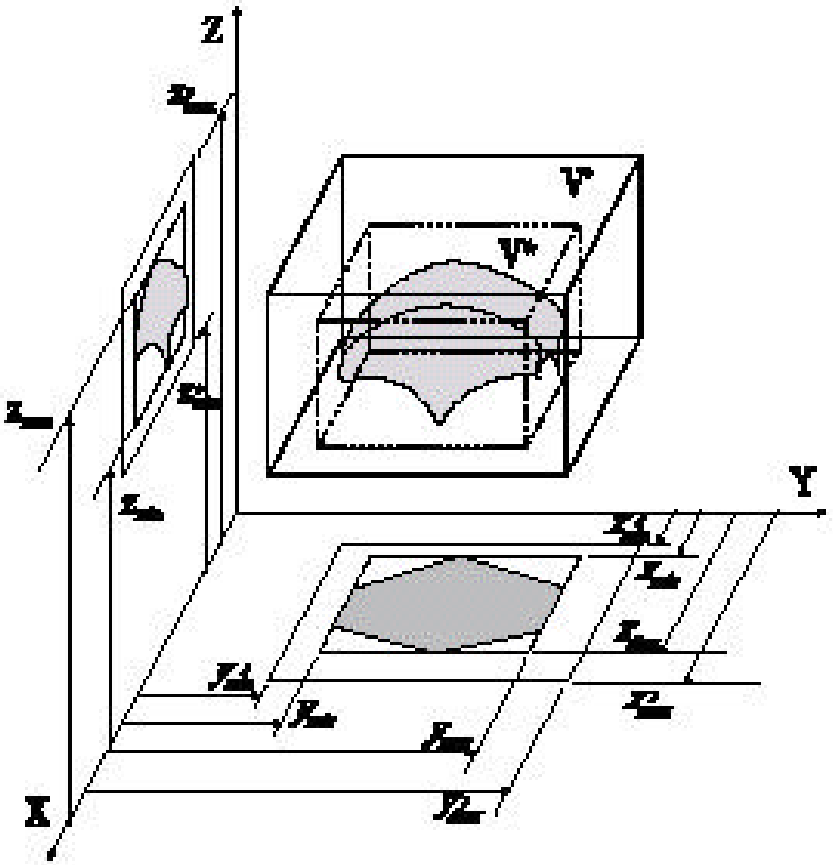

Fig. 1. A numerical approximation for the position workspace volume of CaPaMan manipulator.

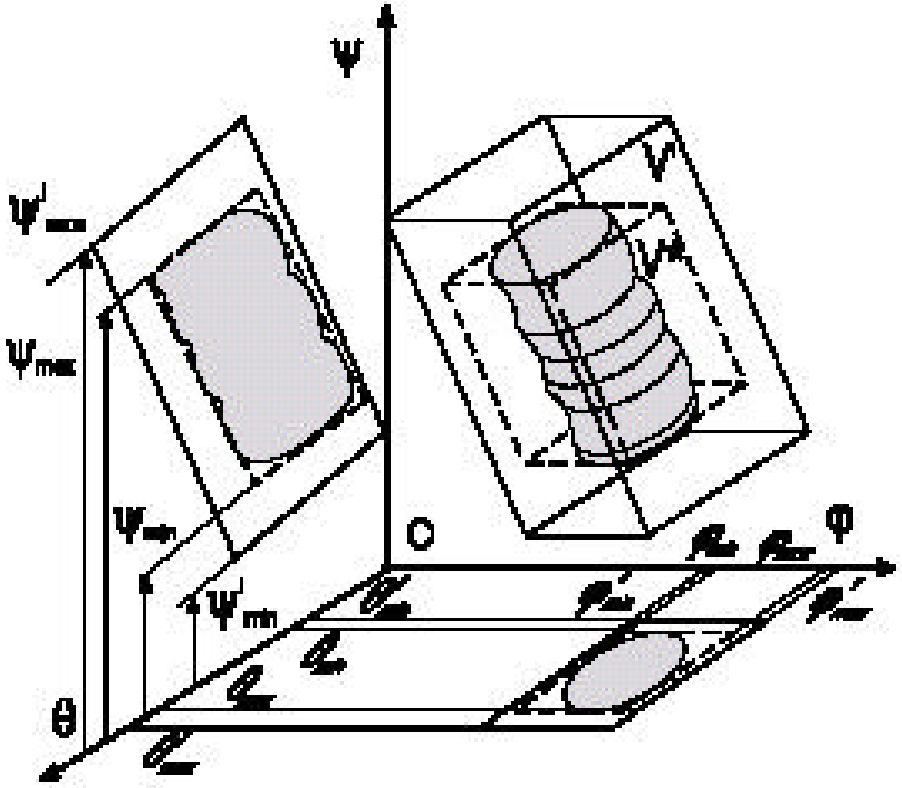

Fig. 2. A numerical approximation for the orientation workspace volume of CaPaMan manipulator.

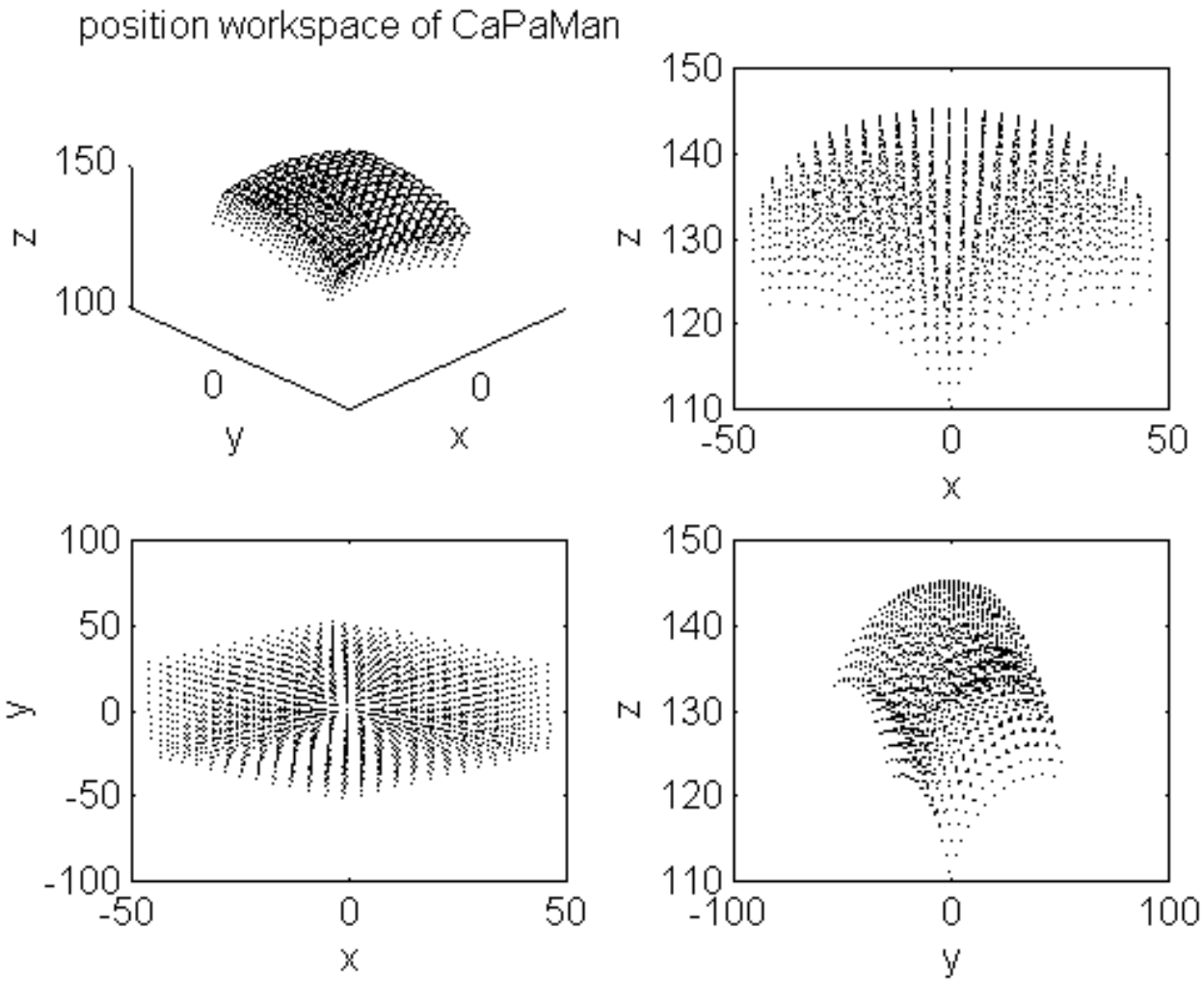

Fig. 3 The position workspace of the optimum designed CaPaMan architecture.

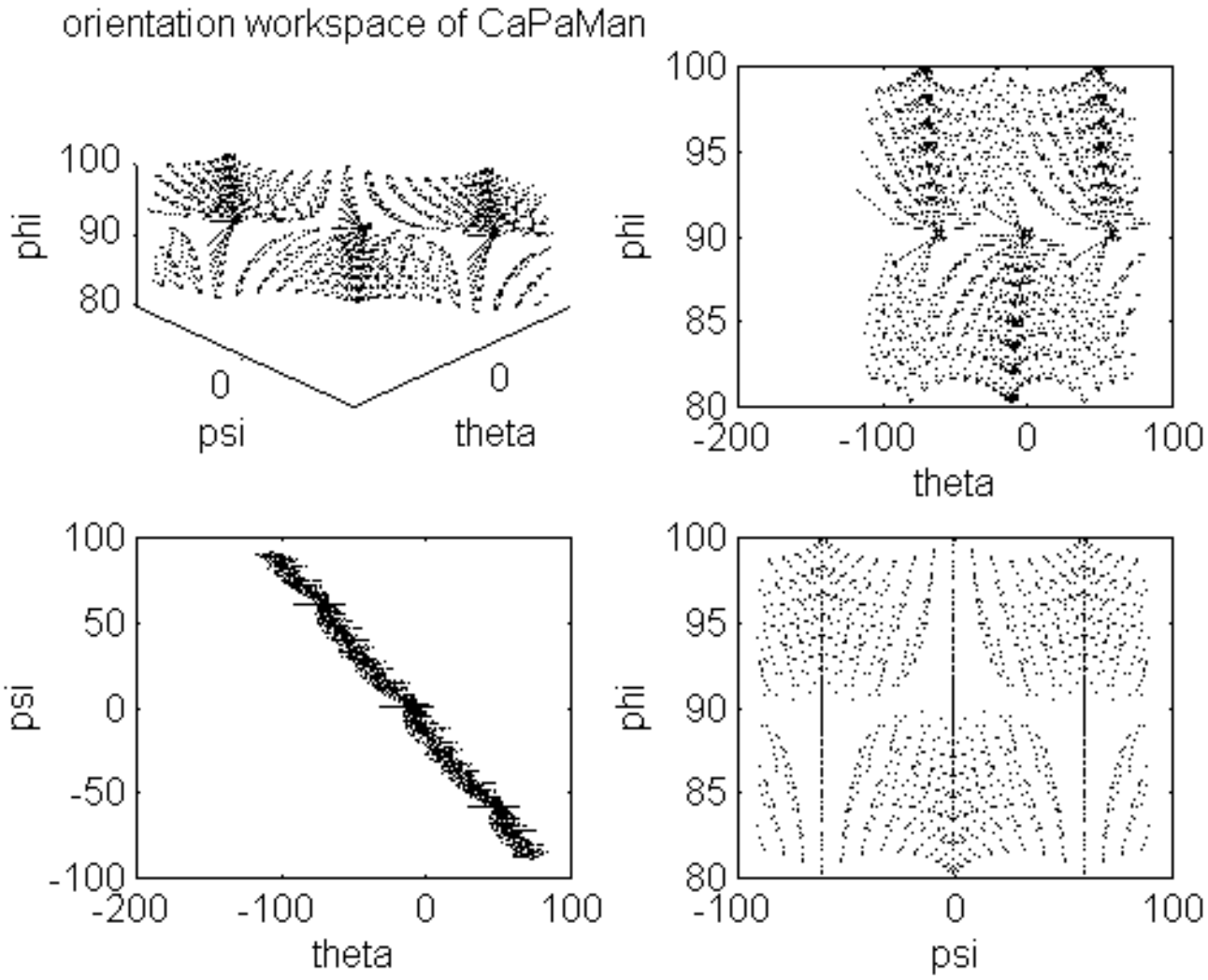

Fig. 4 The orientation workspace of the optimum designed CaPaMan

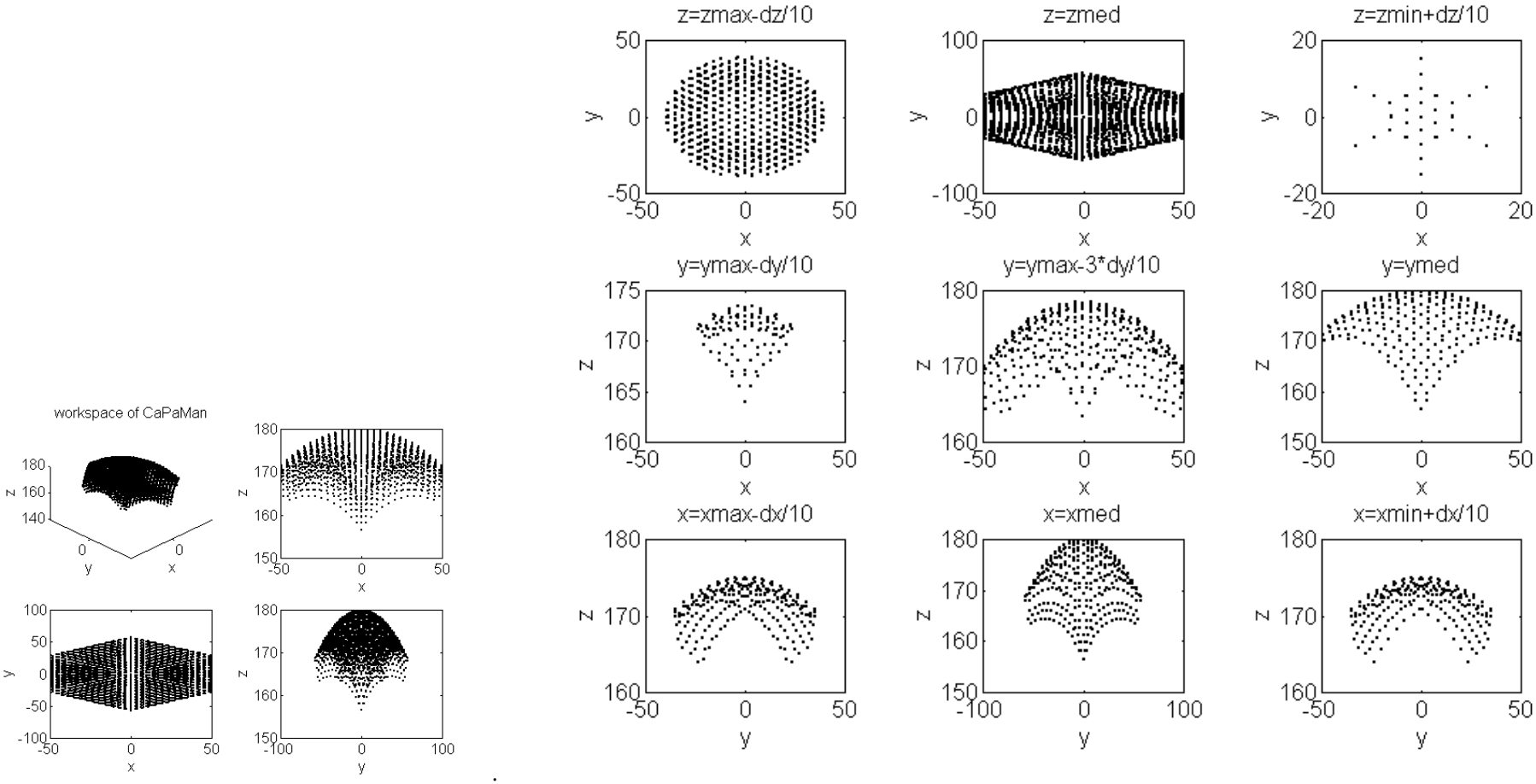

a) b)

Fig.3 Workspace characteristics of CaPaMan prototype, Fig.1 and Table 1 with a scanning interval of 5 deg.: a) position capability; b) workspace sections.

DESIGN PROBLEMS AND FORMULATION

- Several different approaches and algorithms have been presented in the literature
- The strong influence of fundamental characteristics to each other will require to consider those formulations in one design model and nowadays this can be achieved with numerical efficiency by using Optimization Techniques.

the optimum design of parallel manipulators a multi-objective optimization problem can be formulated as

$$\min \mathbf{f}(\mathbf{X}) = \left[f_W(\mathbf{X}), f_S(\mathbf{X}), f_K(\mathbf{X}) \right] \quad (10)$$

Subjected to

$$\mathbf{g}(\mathbf{X}) < \mathbf{0} \quad (11)$$

$$\mathbf{h}(\mathbf{X}) = \mathbf{0}$$

- There are a number of alternative methods to solve numerically a multi-objective optimization problem with Eqs. (10) and (11).
- by using a single objective function F(**X**) and standard constrained optimization methods when the number N of objective components is limited.

$$\min F(\mathbf{X}) = \sum_{\mathbf{i}=1}^{\mathbf{N}} w_i f_i(\mathbf{X}) \quad (12)$$

- w_i are weighting factors, which may correspond or be chosen referring to the relative importance of the objectives.

- the objective functions can be formulated as

$$f_1(X) = \left| 1 - \frac{V_{pos}}{V_{posg}} \right| \quad f_2(X) = \left| 1 - \frac{V_{or}}{V_{org}} \right|$$

$$f_3(X) = \left(1 - \frac{|\Delta x|}{|\Delta x_g|} \right) + \left(1 - \frac{|\Delta y|}{|\Delta y_g|} \right) + \left(1 - \frac{|\Delta z|}{|\Delta z_g|} \right) \quad (13)$$

$$f_4(X) = \left(1 - \frac{|\Delta \varphi|}{|\Delta \varphi_g|} \right) + \left(1 - \frac{|\Delta \psi|}{|\Delta \psi_g|} \right) + \left(1 - \frac{|\Delta \theta|}{|\Delta \theta_g|} \right)$$

$$f_5(X) = \min\left(-\det \mathbf{B}_{nor} \right)$$

The numerical solution of the design problem with Eqs.(12) and (13) can be very cumbersome and even complex when also constraints are considered for assembling operations.

At LARM research activity is carried out and is undergoing to enhance the proposed optimum design formulation for parallel manipulators by using multi-objective optimization and mechanical interpretation of design criteria.
Satisfactory results have been obtained by looking at suitable interpretation of design criteria and analysis formulations, also for experimental tests of validations.

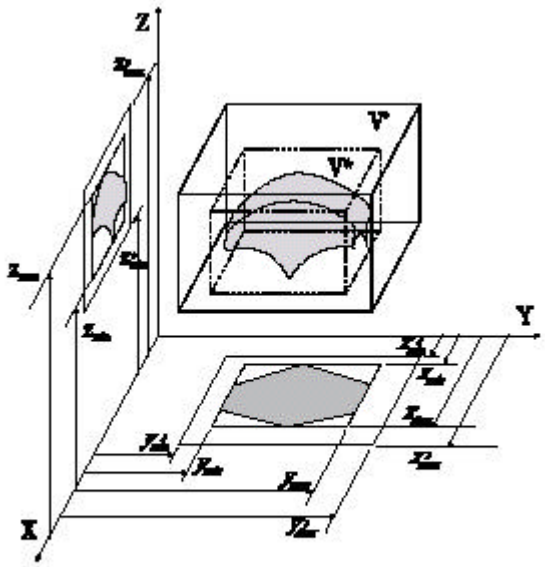

Fig. 1. A numerical approximation for the position workspace volume of CaPaMan manipulator.

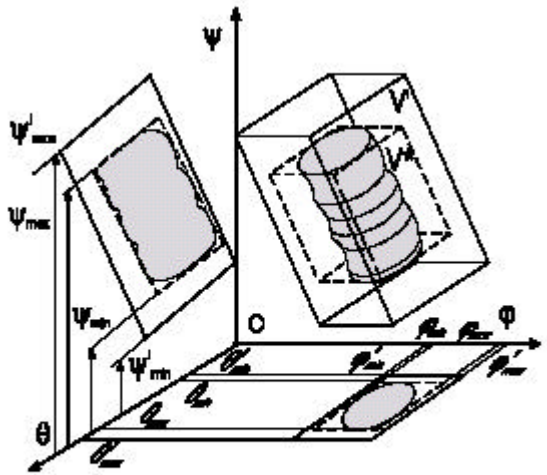

Fig. 2. A numerical approximation for the orientation workspace volume of CaPaMan manipulator.

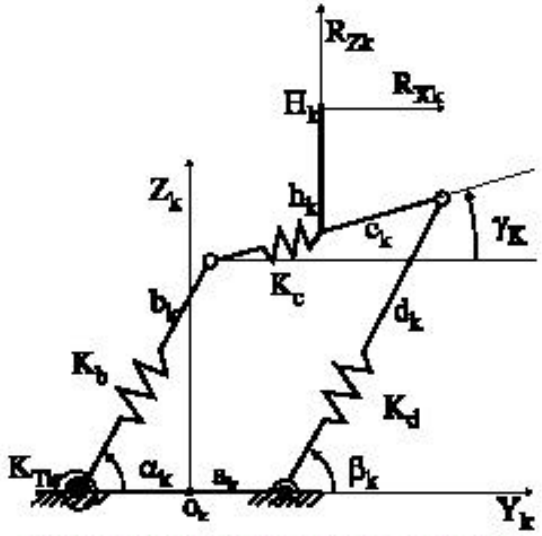

Fig.6 A scheme for stiffness evaluation of a CaPaMan leg.

$$K_{CaPaMan} = M_{FN}\, K_P\, C_P^{-1}\, A_d^{-1}$$

$$G = (9\, r_P^2) / (2 b_k^2)$$

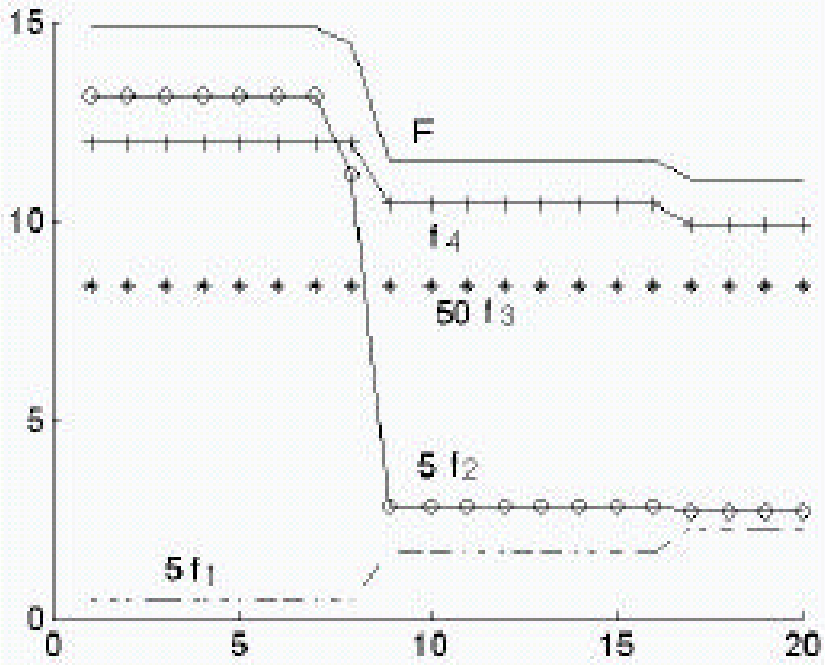

Fig. 7. Evolution of the function F of Eq. (1) and components of Eq. (15) versus number of iterations: position workspace volume as f_1; orientation workspace volume as f_2; compliance displacements and rotations as f_3; singularity condition as f_4.

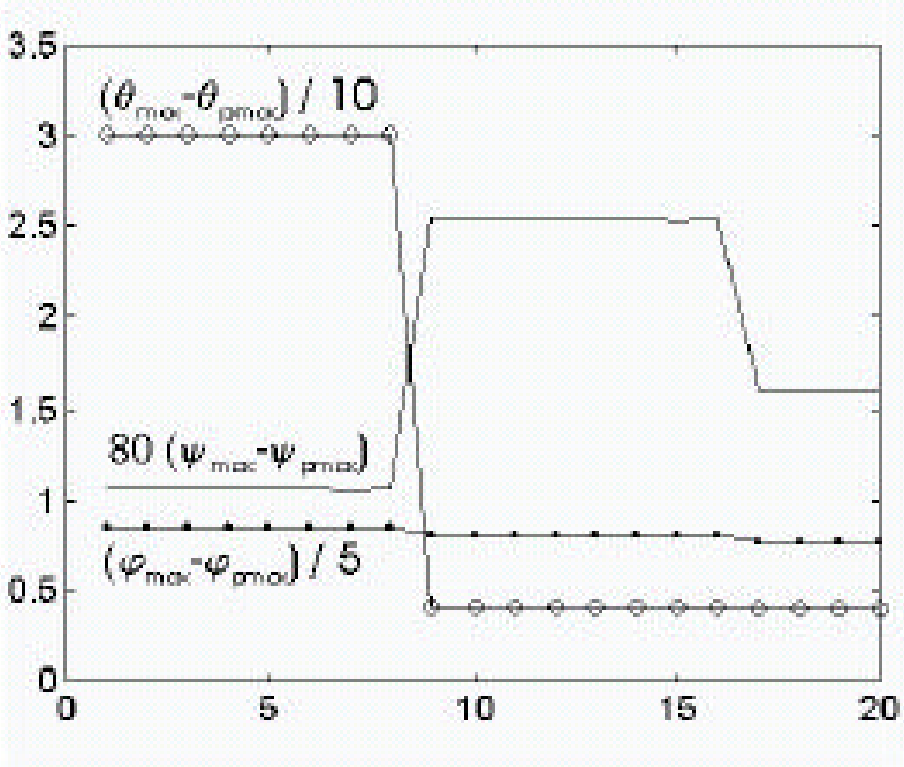

Fig. 8. Evolution of constraints of Eqs. (16) and (17) versus number of iterations for the case of Table 1. (angles are expressed in deg).

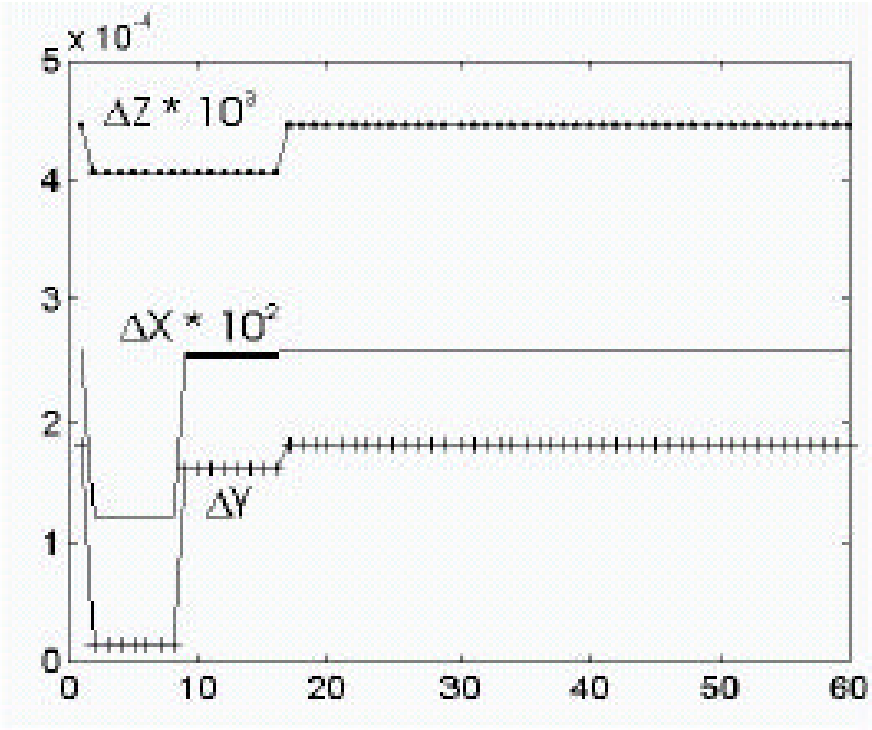

Fig. 9. Evolution of compliance displacements versus number of iterations for the case of Table 1: ΔX, ΔY, and ΔZ; (lengths are expressed in mm).

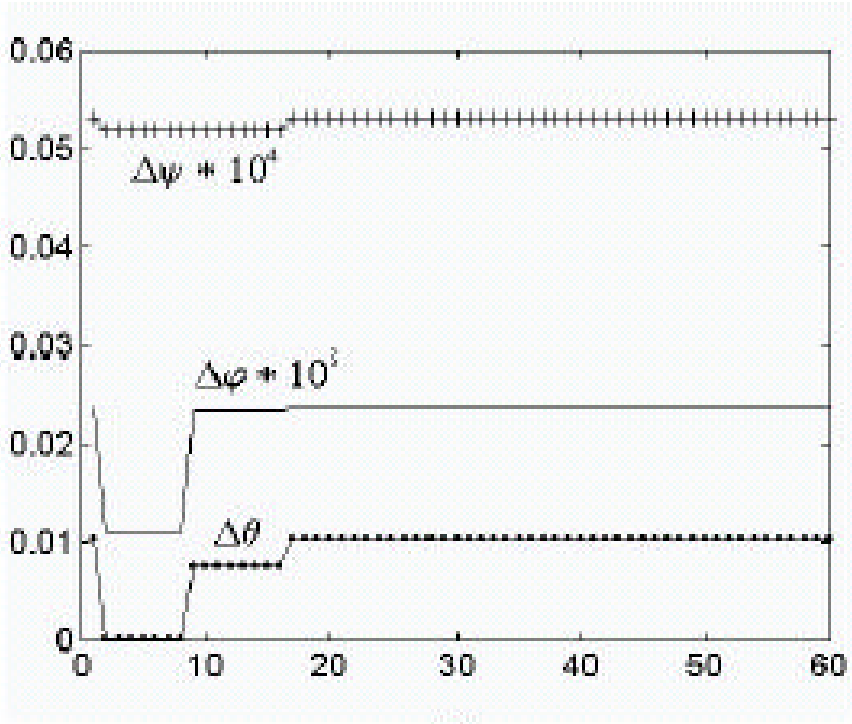

b)

Fig. 10. Evolution of compliance displacements versus number of iterations for the case of Table 1: Δφ, Δψ, and Δθ. (angles are expressed in deg).